All-Optical Pulsed Signal Doppler Frequency Shift Measurement System

Chongjia Huang and Erwin H. W. Chan, *Senior Member, IEEE*

***Abstract*—A simple and all-optical Doppler frequency shift (DFS) measurement system is presented. It is based on a dual-drive Mach Zehnder modulator (DDMZM) driven by a transmitted signal and an echo signal received by an antenna. A low-frequency sawtooth wave is applied to the DDMZM DC port to frequency shift the carrier and sidebands generated by the transmitted signal. Beating of a frequency-shifted transmitted signal sideband and an echo signal sideband at the photodetector produces a low-frequency electrical signal. The DFS, and consequently the speed and moving direction of a target, can be obtained from the frequency of this low-frequency electrical signal. The DDMZM used in the proposed DFS measurement system does not need to be operated at a specific point in the transfer function and hence it has no bias drift problem. The proposed DFS measurement technique can be used in both CW and pulsed radar systems. Experimental results demonstrate the proposed DFS measurement system has a wide operating frequency range of 10 GHz to 19.95 GHz, small DFS measurement error of less than $\pm$0.6 Hz and long-term stable performance. Results also demonstrate, for the first time, DFS measurement of a pulsed signal using a microwave photonic technique.**

***Index Terms*—Serrodyne modulation, frequency translation, doppler frequency, doppler velocity, microwave measurement.**

I. Introduction

THERE is a growing interest in using microwave photonic techniques for radar signal measurement. This arises from wide bandwidth, high measurement speed, low frequency-dependent loss and electromagnetic interference immunity offered by microwave photonics [1], [2]. Among various radar signal parameters, Doppler frequency shift (DFS) is needed in moving target indicator (MTI) and Doppler radar systems, which have numerous military and civilian applications. DFS is the difference between the radar echo and transmitted signal frequency. It is used to obtain the speed and the moving direction of a target. A number of microwave photonic techniques for measuring DFS have been reported. However, they have complex structures that involve multiple laser sources, multiple optical modulators and/or multiple photodetectors (PDs) [3]–[12]. Furthermore, they require electrical components that limit the system operating frequency [3], or an additional microwave reference source that increases the system cost [13]. Many reported techniques rely on measuring the phase difference of two output signals via an oscilloscope to obtain the sign of a DFS in order to determine a target moving direction [3], [6]–[9], [11], [14]. The problem of these techniques is that they can only be used in continuous wave (CW) radar systems. However, many radar systems use pulse modulation.

In this paper, we present a simple single-laser, single-modulator and single-PD based DFS measurement system. It does not involve electrical components and does not require a high-frequency reference signal. It is based on injecting a portion of a transmitted signal and an echo signal received by an antenna to the two RF ports of a dual-drive Mach Zehnder modulator (DDMZM). A low-frequency sawtooth wave is applied to the DDMZM DC bias port to frequency translate the carrier and sidebands generated by the transmitted signal. The frequency of an output electrical signal, generated by beating of the frequency-shifted transmitted signal and echo signal sidebands at the PD, provides information on both the value and sign of DFS. An oscilloscope is not required in the proposed system for DFS measurement. Non-ideal effects due to residual carriers and high order sidebands that can affect the proposed DFS measurement system performance are investigated. Experiments are conducted to verify the DFS measurement capability of the proposed system. Long-term stable performance, and DFS measurement of a pulsed signal and multiple echo signals, are demonstrated.

II. Topology and Operation Principle

The schematic diagram of the proposed DFS measurement system is shown in Fig. 1(a). The system has a simple structure, which consists of a laser, a DDMZM, an optical bandpass filter (OBPF) and a PD. The laser generates CW light, which launches into a DDMZM. The DDMZM consists of a phase modulator on each arm of a Mach Zehnder interferometer (MZI) [15]. It has two RF ports and a DC port. A voltage into the DC port controls the phase difference between the light in the two arms of the MZI. Hence, a DDMZM can be modelled as an MZI containing two phase modulators and a phase shifter, as shown in Fig. 1(b). A portion of a transmitted signal with a frequency f_T is injected to RF Port 1 of the DDMZM. Unlike conventional operation where a DC voltage is applied to the DDMZM DC port, here the DDMZM DC port is driven by a low-frequency sawtooth wave with an amplitude of twice the DDMZM DC port switching voltage. According to the DDMZM model shown in Fig. 1(b), the CW light in the top arm of the DDMZM undergoes phase modulation by the transmitted signal and Serrodyne frequency translation [16], [17]. The amount of frequency translation in

Manuscript received September 6, 2021; revised October 2, 2021; accepted October 5, 2021. Date of publication October 8, 2021; date of current version October 28, 2021. *(Corresponding author: Erwin H. W. Chan.)*

The authors are with the College of Engineering, IT and Environment, Charles Darwin University, Darwin, NT 0909, Australia (e-mail: 1286660746@qq.com; erwin.chan@cdu.edu.au).

Digital Object Identifier 10.1109/JPHOT.2021.3118679

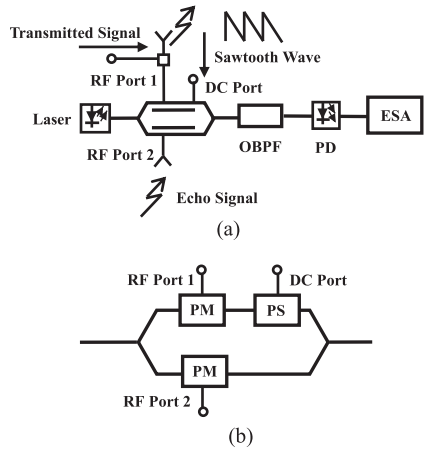

Fig. 1. (a) Structure of the DDMZM based DFS measurement system. (b) Model of a DDMZM. ESA: electrical signal analyser; PM: phase modulator; PS: phase shifter.

the carrier and sidebands of the phase modulated optical signal is the same as the sawtooth wave frequency f_S. An echo signal with a frequency f_E received by an antenna is injected to RF Port 2 of the DDMZM. Therefore, the light travelled in the bottom arm of the DDMZM undergoes phase modulation by the echo signal, according to Fig. 1(b). Hence the output electric field of the DDMZM can be written as

$$E_{DDMZM}(t) = \frac{1}{2}E_{in}\sqrt{t_{ff}}e^{j2\pi f_c t} \times \begin{bmatrix} J_0(m_T)e^{-j2\pi f_S t} + J_1(m_T)e^{j2\pi(f_T-f_S)t} \\ -J_1(m_T)e^{-j2\pi(f_T+f_S)t} + J_0(m_E) \\ +J_1(m_E)e^{j2\pi f_E t} - J_1(m_E)e^{-j2\pi f_E t} \end{bmatrix} \quad (1)$$

where E_{in} and f_c are the electric field amplitude and the frequency of the CW light into the DDMZM respectively, t_{ff} is the insertion loss of the DDMZM, $J_n(x)$ is the Bessel function of nth order of the first kind, $m_T = \pi V_T/V_{\pi,RF}$ and $m_E = \pi V_E/V_{\pi,RF}$ are the modulation index of the transmitted and echo signal respectively, $V_{T(E)}$ is the voltage of the transmitted (echo) signal into the DDMZM and $V_{\pi,RF}$ is the DDMZM RF port switching voltage. (1) shows the output of the DDMZM consists of two sets of optical carrier and sidebands where one set is frequency shifted. An OBPF is connected to the DDMZM output to filter out the optical carrier and the lower sidebands. Hence the output electric field of the OBPF is given by

$$E_{out}(t) = \frac{1}{2}E_{in}\sqrt{t_{ff}}e^{j2\pi f_c t}\left[J_1(m_T)e^{j2\pi(f_T-f_S)t} + J_1(m_E)e^{j2\pi f_E t}\right] \quad (2)$$

The two upper sidebands, generated by the transmitted and echo signals into the DDMZM, are detected by a PD. This produces a photocurrent, which can be expressed as

$$I_{out} = P_{in}t_{ff}\Re\begin{bmatrix} \frac{1}{2}J_1(m_T)J_1(m_E)\cos\left(2\pi(f_E - f_T + f_S)t\right) \\ +\frac{1}{4}\left({J_1}^2(m_T) + {J_1}^2(m_E)\right) \end{bmatrix} \quad (3)$$

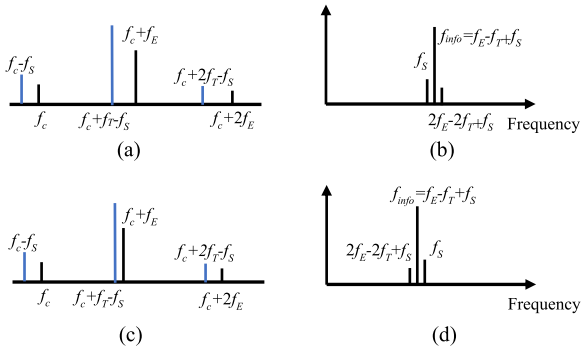

Fig. 2. (a) Optical spectrum after the OBPF and (b) electrical spectrum after the PD for a positive DFS. (c) Optical spectrum after the OBPF and (d) electrical spectrum after the PD for a negative DFS.

where P_{in} is the CW light power into the DDMZM and $\Re$ is the PD responsivity. (3) shows the output photocurrent consists of a DC component and a frequency component at f_E-f_T+f_S. The frequency component at $f_{info} = f_E$-f_T+f_S is referred to as the info peak because f_{info} can be used to determine both the speed and the moving direction of a target. The frequency difference between the info peak and the sawtooth wave is the DFS, i.e., $f_{DFS} = f_{info}$-f_S. Once the value of the DFS is obtained from f_{info}, the speed of a target can be found through the following equation [18].

$$Speed = \frac{|f_{DFS}|\,c}{2f_T\cos\theta} \quad (4)$$

where c is the speed of light in vacuum and θ is the radar elevation angle. The target moving direction can be obtained from the info peak frequency relative to the sawtooth wave frequency. By choosing a sawtooth wave frequency f_S of e.g., 1 MHz, which is much larger than the DFS of $\pm$100 kHz in most applications, if the info peak frequency f_{info} is larger than f_S then $f_{DFS}>0$ and hence the target is moving toward the radar. On the other hand, if f_{info} is smaller than f_S then $f_{DFS}<0$ and hence the target is moving away from the radar.

In practice, the magnitude response of an OBPF has a finite edge roll off, which causes small amount of the optical carrier with and without being frequency shifted, to pass through the OBPF, and higher order sidebands are generated at the DDMZM output. By including these two non-ideal effects in the analysis, the system output electric field into the PD becomes

$$E_{out}(t) = \frac{1}{2}E_{in}\sqrt{t_{ff}}e^{j2\pi f_c t} \times \begin{bmatrix} \sqrt{\alpha}\left(J_0(m_T)e^{-j2\pi f_S t} + J_0(m_E)\right) \\ +J_1(m_E)e^{j2\pi f_E t} + J_1(m_T)e^{j2\pi(f_T-f_S)t} \\ +J_2(m_E)e^{j2\pi(2f_E)t} + J_2(m_T)e^{j2\pi(2f_T-f_S)t} \end{bmatrix} \quad (5)$$

where α is the amount of suppression introduced by the OBPF at around the optical carrier frequency. Since the lower sidebands are far away from the upper sidebands, they are largely suppressed by the OBPF and hence they are neglected in the analysis. Fig. 2(a) and 2(c) show the output optical spectrum

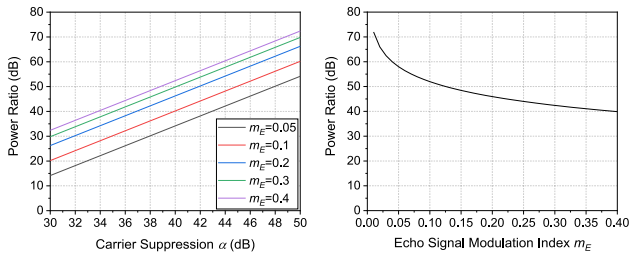

Fig. 3. (a) Simulated power ratio of the info peak at f_E-f_T+f_S to the unwanted peak at f_S versus the amount of suppression α introduced by the OBPF at around the optical carrier frequency for different echo signal modulation indexes m_E. (b) Simulated power ratio of the info peak at f_E-f_T+f_S to the unwanted peak at $2f_E$-$2f_T$+f_S for different echo signal modulation indexes m_E when the transmitted signal modulation index m_T is fixed at 0.4.

obtained based on (5) for a positive and negative DFS respectively. Beating of the optical frequency components shown in Fig. 2(a) and 2(c) at the PD generates photocurrents at different frequencies. Fig. 2(b) and 2(d) shows the electrical spectrum after the PD at around the info peak frequency $f_{info} = f_E$-f_T+f_S for a positive and negative DFS respectively. This shows the non-ideal effects generate two unwanted peaks at f_S and $2f_E$-$2f_T$+f_S around the info peak. The photocurrent at the info peak frequency is the same as that given in the first term inside the square brackets in (3). The photocurrents at the two unwanted peak frequencies can be obtained from (5) and are given by

$$I_{f_S} = \frac{1}{2}\alpha P_{in} t_{ff} \Re J_0(m_T) J_0(m_E) \cos(2\pi f_S t) \quad (6)$$

$$I_{2f_E-2f_T+f_S} = \frac{1}{2} P_{in} t_{ff} \Re J_2(m_T) J_2(m_E) \times \cos\left(2\pi(2f_E - 2f_T + f_S)t\right) \quad (7)$$

The amplitudes of the two unwanted peaks need to be much smaller than the info peak amplitude to avoid errors in DFS measurement such as identifying a non-existing object. Although the existence of the unwanted peak at f_S does not indicate there is a moving object, it could cause measurement error when using a frequency counter to measure the info peak frequency. The electrical power ratio of the info peak to the unwanted peaks at f_S and $2f_E$-$2f_T$+f_S are given by

$$\frac{P_{f_{info}}}{P_{f_S}} = \left(\frac{J_1(m_T)J_1(m_E)}{\alpha J_0(m_T)J_0(m_E)}\right)^2 \quad (8)$$

$$\frac{P_{f_{info}}}{P_{2f_E-2f_T+f_S}} = \left(\frac{J_1(m_T)J_1(m_E)}{J_2(m_T)J_2(m_E)}\right)^2 \quad (9)$$

III. Simulation Results and Discussion

Fig. 3(a) shows the power ratio of the info peak at f_E-f_T+f_S to the unwanted peak at f_S for different amount of suppression α introduced by the OBPF at around the optical carrier frequency. It was plotted using (8) with a transmitted signal modulation index m_T of 0.4. This shows, in order to ensure the unwanted peak at f_S is more than 30 dB below the info peak, the carrier with and without frequency shift need to be suppressed by more than 32 dB and the echo signal modulation index needs to be larger than 0.2 when the transmitted signal modulation index is 0.4. Fig. 3(b) shows the unwanted peak at $2f_E$-$2f_T$+f_S is around 40 dB below the info peak when both the transmitted and echo signal modulation indexes are 0.4. This also shows, the smaller the echo signal modulation index is, the smaller the unwanted peak power at $2f_E - 2f_T + f_S$ becomes.

Note that using a DDMZM for DFS measurement has been reported [13], [14]. The DFS measurement system presented in [13] requires a reference signal at around the transmitted signal frequency. A microwave signal generator is needed for generating a reference signal at a microwave frequency, which increases the system cost. Furthermore, an electrical power combiner is needed to combine the reference and transmitted signals before injecting to the DDMZM. The use of an electrical component limits the system bandwidth. The DFS measurement system presented in [14] has the same structure but totally different operation principle compared to the proposed DFS measurement system. Although a sawtooth wave is shown at the input of the DDMZM DC port in [14], it is not used for frequency translation. Instead the sawtooth wave is used to indicate a time-varying optical phase difference is introduced to the two arms of the DDMZM. The experimental results presented in [14] are obtained by switching two bias states of the DDMZM via a DC power supply rather than applying a sawtooth wave to the DDMZM. Switching the DDMZM bias state changes the phase of the output waveform. By using an oscilloscope to monitor the phase shift of the output waveform caused by changing the DDMZM bias voltage, the sign of the DFS and consequently the target moving direction can be determined. As was discussed in Section I, this technique not only needs an oscilloscope in addition to an electrical signal analyser (ESA) for DFS measurement, it cannot be used for measuring DFS of a pulsed signal or multiple echo signals.

The proposed DFS measurement system does not require the DDMZM to be operated at a specific point in the transfer function. Therefore, unlike all reported microwave photonic based DFS measurement systems, it has the advantage of no bias drift problem. Note that only the info peak frequency, which can be measured on a frequency counter or a low-frequency ESA, is needed to determine a target speed and moving direction. Using a low-frequency ESA to measure the info peak frequency has the advantage of suppressing the optical carriers at f_c and f_c-f_S is not necessary. This is because beating of the optical carrier with and without frequency shift at the PD generates a frequency component at the input sawtooth wave frequency f_S, which does not contain information of a moving object. Hence, it can be neglected. Since optical carrier suppression is not required, the OBPF only needs to suppress one of the sidebands. The lower operating frequency of the DFS measurement system can be extended to around 3 GHz when using a high edge roll off OBPF for sideband suppression. A frequency counter can provide a low cost and compact solution for measuring the info peak frequency. However, this requires the optical carrier to be largely suppressed so that the info peak is the dominant frequency component at the system output. This limits the DFS measurement system lower operating frequency due to the OBPF has a finite edge roll off.

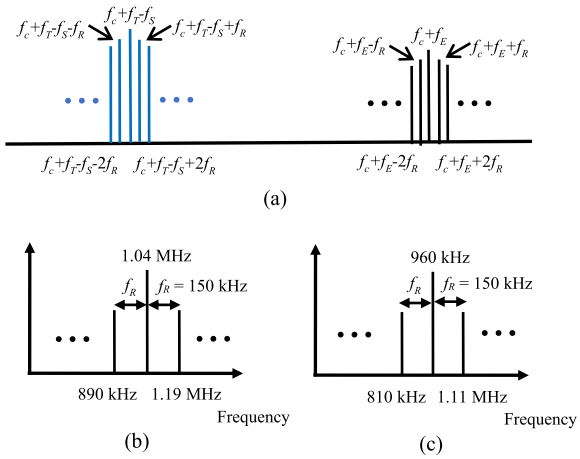

Fig. 4. (a) DDMZM based DFS measurement system output optical spectrum when the transmitted signal is pulse modulated. System output electrical spectrum for a DFS of (b) +40 kHz and (c) -40 kHz. The sawtooth wave frequency is 1 MHz and the transmitted signal pulse repetition frequency is 150 kHz.

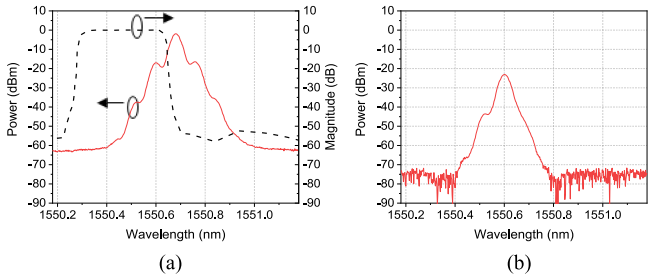

Fig. 5. Measured optical spectrum (a) before and (b) after the tunable OBPF when the DDMZM was driven by a 10 GHz transmitted signal and a 10 GHz + 50 kHz echo signal. Normalised magnitude response of the tunable OBPF (dashed line).

The proposed DDMZM based DFS measurement system can be used in pulsed radar systems. In this case, the transmitted and echo signals are infinite train of pulses. Their spectrums compose of discrete spectral lines with line spacing equal to the pulse repetition frequency f_R. Fig. 4(a) shows the output optical spectrum of the proposed structure used in a pulsed radar system. Note that only five spectral lines generated by the transmitted and echo pulsed signals are shown in the figure. The residual optical carriers and the second order sidebands are not shown in the figure for simplicity. Beating of the spectral lines at the PD generates an output electrical spectrum, which consists of the info peak at $f_{info} = f_E$-f_T+f_S and peaks at nf_R and f_E-f_T+f_S±nf_R where n is an integer. By choosing the pulse repetition frequency f_R to be twice the possible DFS f_{DFS} to avoid Doppler ambiguity, the info peak must be located within f_S±f_R/2 where the values of both f_S and f_R are known and can be designed to suit different applications. This shows, although the output spectrum consists of a number of peaks, under an ideal situation, there is only one peak within the frequency range of f_S±f_R/2 and this peak is the info peak. Note that the proposed DFS measurement system does not require time synchronisation because it only involves frequency measurement. Furthermore, the transmitter and the receiver are located on the same platform, which can share the same frequency source.

Considering an example where a radar system is transmitting an 8 GHz pulsed signal with a pulse repetition frequency of 150 kHz. A sawtooth wave with a frequency of 1 MHz is used in the DDMZM based DFS measurement system. Fig. 4(b) and 4(c) show the system output electrical spectrum for a DFS of +40 kHz and -40 kHz respectively. As shown in the figures, there is a peak with the highest amplitude at around the sawtooth wave frequency of 1 MHz. This is the info peak and is located at the frequency of f_E-f_T+f_S, i.e., 1.04 MHz in Fig. 4(b) and 960 kHz in Fig. 4(c). As in the CW system, the value and the sign of the DFS can be obtained from the difference between the info peak frequency and the sawtooth wave frequency. The figures also show, under an ideal situation, the info peak is the only frequency component present in the frequency range of f_S±f_R/2 = 1 MHz ± 75 kHz.

IV. Experimental Results

An experiment based on the structure shown in Fig. 1(a) was set up to verify the DDMZM based DFS measurement system. The laser source was a tunable laser (Keysight N7711A). It generated a narrow-linewidth CW light with 1550 nm wavelength and 10 dBm optical power. The CW light was launched into a DDMZM (Fujitsu FTM7937). A 10 GHz transmitted signal and a 10 GHz + 50 kHz echo signal, which were generated by two microwave signal generators (Analog Devices HMC-T2220 and Keysight N5173B), were applied to the two RF ports of the DDMZM. The modulation indexes of the transmitted and echo signals were set at 0.4 and 0.2 respectively. The DDMZM DC port was driven by a 1 MHz sawtooth wave with a negative slope generated by a waveform generator (Rigol DG4202). The peak-to-peak voltage of the sawtooth wave was set at 5.7 V, which is around twice the DDMZM DC port switching voltage, to minimise the loss of the frequency translation process. The fall time to period ratio of the sawtooth wave was measured to be 0.7%. Hence, according to [16], spurious signals produced by the frequency translation process are more than 40 dB below the frequency shifted signal. A tunable OBPF (Alnair Labs BVF-300CL) was connected to the DDMZM output. The filter centre wavelength and bandwidth were adjusted to pass only one sideband. An erbium-doped fibre amplifier (EDFA) (Amonics AEDFA-PA-35-B-FA) and a 0.5 nm 3-dB bandwidth optical filter were employed to compensate for the system loss and to suppress the amplified spontaneous emission noise. The output optical signal, which had an average optical power of 6 dBm, was detected by a PD (Discovery Semiconductor DSC30S). An ESA (Keysight N9000A) was connected to the PD output to measure the info peak frequency. The ESA, the two microwave signal generators and the waveform generator were synchronised via a common 10 MHz reference.

The optical spectrum before and after the tunable OBPF were measured on an optical spectrum analyser (OSA) (Anritsu MS9740A) and are shown in Fig. 5(a) and 5(b) respectively. Fig. 5(a) also shows the measured tunable OBPF magnitude

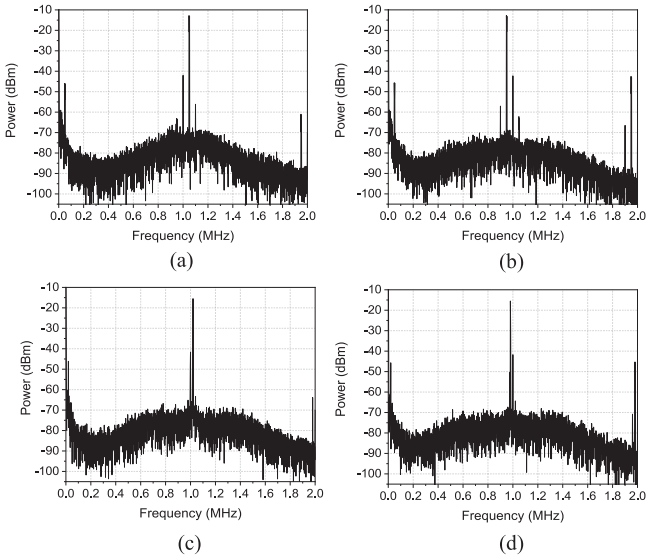

Fig. 6. Measured electrical spectrum at the output of the DDMZM based DFS measurement system for a 10 GHz transmitted signal and an echo signal with a frequency of (a) 10 GHz + 50 kHz and (b) 10 GHz - 50 kHz, and a 19.95 GHz transmitted signal and an echo signal with a frequency of (c) 19.95 GHz + 20 kHz and (d) 19.95 GHz - 20 kHz.

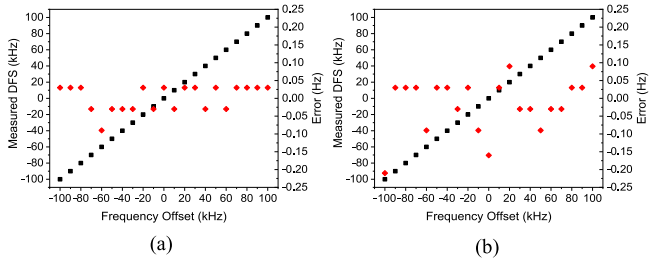

Fig. 7. Measured DFS (black square) and the corresponding DFS measurement error (red diamond) versus the echo signal frequency offset. The transmitted signal frequency is (a) 10 GHz and (b) 19.95 GHz.

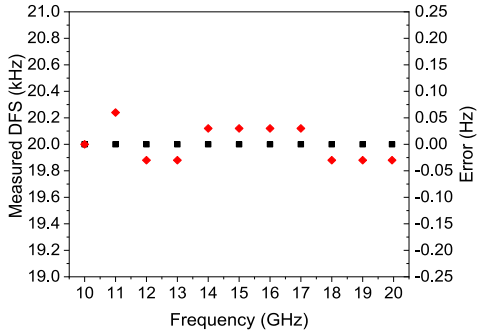

Fig. 8. Measured DFS (black square) and the corresponding DFS measurement error (red diamond) versus the transmitted signal frequency.

response. Note that the horizontal axis on the OSA display is in wavelength. As shown in the figure, the lower sidebands in wavelength, which correspond to the upper sidebands in frequency, pass through the tunable OBPF. Fig. 6(a) and 6(b) show the DFS measurement system output electrical spectrums when the echo signal frequency is 10 GHz + 50 kHz and 10 GHz - 50 kHz, respectively. It can be seen from the figure that there are four peaks at around the sawtooth wave frequency. The peak with an amplitude of around 30 dB higher than the other peaks is the info peak. It is located at 1.05 MHz in Fig. 6(a) and 950 kHz in Fig. 6(b), which indicate the DFS is +50 kHz and -50 kHz, respectively, since the sawtooth wave frequency is 1 MHz. According to (4), a DFS of +50 kHz and -50 kHz indicate the target is moving with a speed of 750/cosθ m/s toward and away from the radar respectively. The peak with the second highest amplitude is located at the sawtooth wave frequency of 1 MHz and is due to the residual optical carrier with and without being frequency shifted pass through the tunable OBPF. The next highest peak, which is located at 1.1 MHz in Fig. 6(a) and 900 kHz in Fig. 6(b), is due to the transmitted and echo signal second order sidebands, which can be seen in Fig. 5(b). The present of these peaks was discussed in Section II. The peak with the smallest amplitude at around the sawtooth wave frequency is generated by the beating of the echo signal sideband at f_c+f_E and the spurious signal at f_c+f_T+f_S produced by the non-ideal frequency translation process, at the PD. The peaks at around DC and 2 MHz are outside the possible frequency range of the info peak and hence can be neglected. The transmitted and echo signal frequencies were changed to 19.95 GHz and 19.95 GHz ± 20 kHz to demonstrate the DFS measurement system is capable to operate at higher frequencies. The system output electrical spectrums are shown in Fig. 6(c) and 6(d). This shows the dominant frequency component, which is the info peak, is located at 1.02 MHz and 980 kHz when the echo signal frequency is 19.95 GHz + 20 kHz and 19.95 GHz - 20 kHz respectively. A DFS of ±20 kHz can be obtained from the info peak frequency. As in Fig. 6(a) and 6(b), there are three unwanted peaks around the info peak and they are more than 25 dB below the info peak.

Fig. 7(a) shows the DFS obtained from the difference between the info peak frequency measured on the ESA and the sawtooth wave frequency, for different echo signal frequency offsets when the transmitted signal at 10 GHz. The measurement error, which is obtained by comparing the DFS with the frequency offset on the two microwave signal generators, is also shown in the figure. It can be seen from the figure that the DFS measurement error is within ±0.1 Hz for the echo signal with a frequency between 10 GHz ± 100 kHz. The same measurement was performed after changing the transmitted signal frequency from 10 GHz to 19.95 GHz. As shown in Fig. 7(b), the DFS measurement error is within ±0.22 Hz over the echo signal frequency offset of ±100 kHz. The performance of the DDMZM based DFS measurement system at different operating frequencies was investigated. This was done by measuring the info peak frequency on the ESA for different transmitted signal frequencies, while the echo signal frequency offset was fixed at +20 kHz. The DFS and the corresponding DFS measurement error are shown in Fig. 8. It can be seen from the figure that the measurement error is within the range of -0.03 Hz to 0.06 Hz for the transmitted signal frequency of 10 GHz to 19.95 GHz. The upper operating frequency was limited by the frequency range of the microwave

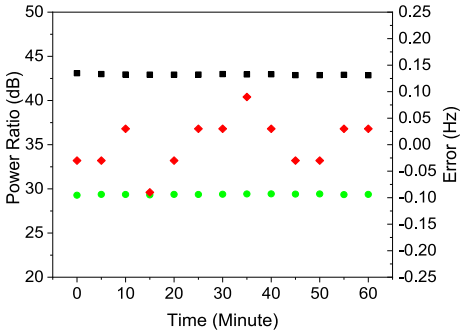

Fig. 9. Power ratio of the info peak at 1.01 MHz to the unwanted peak at 1 MHz (green dot) and 1.02 MHz (black square), and the DFS measurement error (red diamond) versus time, for a 10 GHz transmitted signal and a 10 GHz + 10 kHz echo signal into the DDMZM.

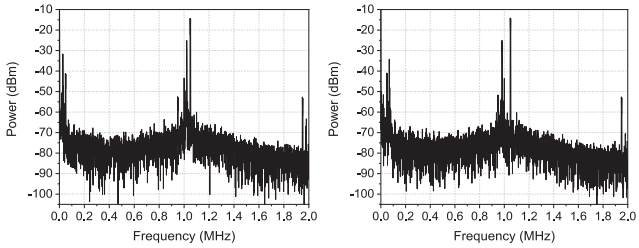

Fig. 10. Measured system output electrical spectrum for a 10 GHz transmitted signal, and two echo signals with frequencies of (a) 10 GHz + 50 kHz and 10 GHz + 20 kHz, and (b) 10 GHz + 50 kHz and 10 GHz - 20 kHz, into the DDMZM.

signal generators used in the experiment. The lower operating frequency of 10 GHz was used to ensure that the info peak is more than 25 dB above the adjacent unwanted peaks.

The power ratio of the info peak to the two highest-amplitude unwanted peaks, and the DFS measurement error obtained from the info peak frequency, were recorded every 5 minutes over an hour to investigate the system stability. The frequencies of the transmitted and echo signals were set at 10 GHz and 10 GHz + 10 kHz respectively. Fig. 9 shows the unwanted peaks at 1 MHz and 1.02 MHz are 29 dB and 43 dB below the info peak at 1.01 MHz respectively. More importantly, there is less than 0.3 dB change in the power ratio of the info peak to the unwanted peaks during the one-hour measurement period. Fig. 9 also shows the DFS measurement error remains within ±0.1 Hz over an hour. This demonstrates the proposed DFS measurement system, in which the DDMZM does not require a DC bias voltage, has a long-term stable performance.

Two different-frequency echo signals were applied to the DDMZM to demonstrate the proposed system has the ability to measure DFS of multiple echo signals. The two echo signals were generated by a microwave signal generator (Keysight N5173B) and a network analyser (Keysight E5063). They had different frequencies and powers, and were combined by a power combiner (Gwave GPD-2-020265) before being applied to the DDMZM through the modulator RF Port 2. RF Port 1 of the DDMZM was driven by a 10 GHz transmitted signal. Fig. 10(a) shows the system output electrical spectrum when the two echo signal frequencies are 10 GHz + 50 kHz and 10 GHz + 20 kHz.

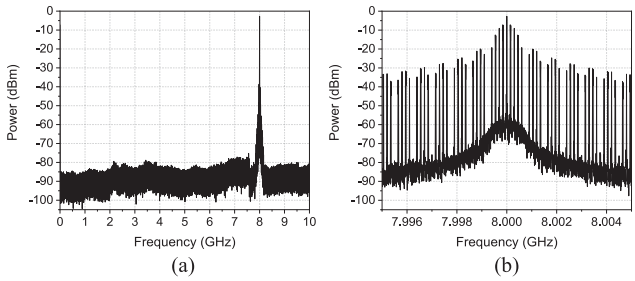

Fig. 11. (a) Transmitted pulsed signal spectrum measured in a 10 GHz span. (b) Detailed section of the spectrum within 10 MHz of the transmitted signal frequency.

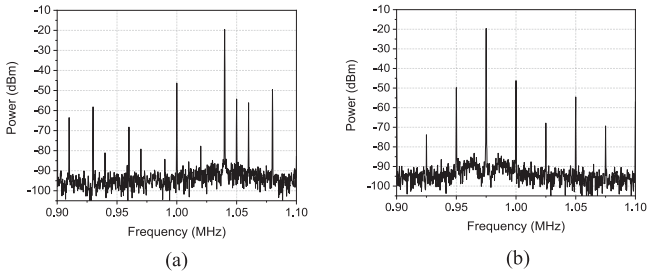

Fig. 12. Measured system output electrical spectrum for an 8 GHz transmitted pulsed signal with a pulse repetition frequency of 150 kHz and an echo signal with (a) +40 kHz and (b) -25 kHz frequency offset.

As shown, there are two dominant peaks at around the sawtooth wave frequency of 1 MHz. They are the two info peaks, which have the frequencies of 1.02 MHz and 1.05 MHz. This indicates that the DFS of the two echo signals are +20 kHz and +50 kHz. Note that the two info peaks are over 18 dB higher than the unwanted peak at the 1 MHz sawtooth wave frequency and are over 27 dB higher than the unwanted peak at 950 kHz generated by the beating of the second order sidebands at the PD. The frequency of the 10 GHz + 20 kHz echo signal was changed to 10 GHz - 20 kHz. As shown in Fig. 10(b), the frequencies of the two info peaks become 980 kHz and 1.05 MHz. The power ratio of the info peak to the unwanted peaks are the same as that shown in Fig. 10(a). Therefore, the number of echo signals, which leads to the number of moving targets, can be obtained from the number of dominant peaks at around the sawtooth wave frequency. The speed and moving direction of each target can be found from the info peak frequencies.

A transmitted pulsed signal and an echo pulsed signal were used to demonstrate the proposed system can measure the DFS of a pulsed signal. Each of the two pulsed signals was generated by mixing a CW signal from a microwave signal generator with a 150 kHz repetition frequency pulse train from a dual-output waveform generator (Rigol DG4102), via an electrical mixer. The carrier frequency of the transmitted pulsed signal was 8 GHz. Fig. 11 shows the transmitted pulsed signal spectrum has multiple spectral lines separated by 150 kHz pulse repetition frequency and is centred at 8 GHz. Fig. 12(a) shows the DDMZM based DFS measurement system output electrical spectrum when the echo pulsed signal has a centre frequency of 8 GHz + 40 kHz. As was discussed in Section III, since the sawtooth wave frequency is $f_S = 1$ MHz and the pulse repetition

frequency is $f_R = 150$ kHz, the info peak must be located within $f_S \pm f_R/2$, i.e., 925 kHz and 1.075 MHz. Fig. 12(a) shows there are several peaks in this frequency range but only one peak has a dominant amplitude. This info peak is located at 1.04 MHz. A similar output electrical spectrum was obtained as shown in Fig. 12(b) when the echo pulsed signal centre frequency was changed to 8 GHz - 25 kHz. In this case, the dominant peak, i.e., the info peak, is located at 975 kHz. The results in Fig. 12(a) and 12(b) show the proposed microwave photonic technique for DFS measurement can be used in pulsed radar systems.

V. Conclusion

A new microwave photonic based DFS measurement system has been presented. It is based on using Serrodyne frequency translation to frequency shift a transmitted signal sideband, which beats with an echo signal sideband at a PD to generate a low-frequency electrical signal. Both the value and the sign of DFS, and consequently the speed and the moving direction of a target, can be obtained from the frequency difference between this low-frequency electrical signal and the sawtooth wave that is used for frequency translation. This eliminates using an oscilloscope, which is needed in most reported microwave photonic based DFS measurement systems, to determine the target moving direction. The proposed DFS measurement system has a simple structure and is free of electrical components. Furthermore, no DC bias voltage is required to bias the DDMZM used in the system at a specific point in the transfer function. Only a low-frequency sawtooth wave, which can be produced by a low-cost waveform generator, is needed for the frequency translation process. Experimental results show the DFS measurement error is less than ± 0.06 Hz for a 10 to 19.95 GHz transmitted signal frequency and an echo signal with $+20$ kHz frequency offset. DFS measurement error remains below ± 0.1 Hz and the power ratio of the info peak to the unwanted peak has less than 0.3 dB change during a one-hour measurement period, demonstrating the system has a long-term stable performance. Results also demonstrate DFS measurement of two different-frequency echo signals and a pulsed signal with a 150 kHz pulse repetition frequency.

References

[1] S. Pan and J. Yao, "Photonics-based broadband microwave measurement," *J. Lightw. Technol.*, vol. 35, no. 16, pp. 3498–3513, Aug. 2017.

[2] X. Zou, B. Lu, W. Pan, L. Yan, and J. Yao, "Photonics for microwave measurements," *Laser Photon. Rev.*, vol. 10, no. 5, pp. 711–734, 2016.

[3] X. Li *et al.*, "Photonic doppler frequency shift measurement based on a dual-polarization modulator," *App. Lett.*, vol. 56, no. 8, pp. 2084–2089, 2017.

[4] X. Zou, W. Li, B. Lu, W. Pan, L. Yan, and L. Shao, "Photonic approach to wide-frequency-range high-resolution microwave/millimeter-wave doppler frequency shift estimation," *IEEE Trans. Microw. Theory Techn.*, vol. 63, no. 4, pp. 1421–1430, Apr. 2015.

[5] B. Lu, W. Pan, X. Zou, X. Yan, L. Tan, and B. Luo, "Wideband doppler frequency shift measurement and direction ambiguity resolution using optical frequency shift and optical heterodyning," *Opt. Lett.*, vol. 40, no. 10, pp. 2321–2324, 2015.

[6] B. Lu *et al.*, "Wideband microwave doppler frequency shift measurement and direction discrimination using photonic I/Q detection," *J. Lightw. Technol.*, vol. 34, no. 20, pp. 4639–4645, Oct. 2016.

[7] W. Chen *et al.*, "Wideband doppler frequency shift measurement and direction discrimination based on a DPMZM," *IEEE Photon. J.*, vol. 9, no. 2, Apr. 2017, Art. no. 5501008.

[8] F. Zhang, J. Shi, and S. Pan, "Photonics-based wideband doppler frequency shift measurement by in phase and quadrature detection," *Electron. Lett.*, vol. 54, no. 11, pp. 708–710, 2018.

[9] B. Kang *et al.*, "6-40 GHz photonic microwave doppler frequency shift measurement based on polarization multiplexing modulation and I/Q balanced detection," *Opt. Commun.*, vol. 456, 2020, Art. no. 124579.

[10] H. Zhuo, A. Wen, and Z. Tu, "Photonic doppler frequency shift measurement without ambiguity based on cascade modulation," *Opt. Commun.*, vol. 470, 2020, Art. no. 125798.

[11] C. Yi, H. Chi, and T. Jin, "A photonic approach for doppler frequency shift measurement with dispersion medium," *IEEE Photon. J.*, vol. 12, no. 5, Oct. 2020, Art. no. 7102708.

[12] C. Huang, E. H. W. Chan, and C. B. Albert, "Wideband DFS measurement using a low-frequency reference signal," *IEEE Photon. Technol. Lett.*, vol. 31, no. 20, pp. 1643–1646, Oct. 2019.

[13] L. Xu, Y. Yu, H. Tang, and X. Zhang, "A simplified photonic approach to measuring the microwave doppler frequency shift," *IEEE Photon. Technol. Lett.*, vol. 30, no. 3, pp. 246–249, Feb. 2018.

[14] Y. Yang, Y. Xiang, Z. Tang, and S. Pan, "Photonic method for microwave doppler frequency shift measurement based on an auxiliary phase shift," in *Proc. Asia Commun. Photon. Conf.*, 2019, Art. no. T3E.2.

[15] K. P. Ho and H. W. Cuei, "Generation of arbitrary quadrature signals using one dual-drive modulator," *J. Lightw. Technol.*, vol. 23, no. 2, pp. 764–770, Feb. 2005.

[16] L. M. Johnson and C. H. Cox, "Serrodyne optical frequency translation with high sideband suppression," *J. Lightw. Technol.*, vol. 6, no. 1, pp. 109–112, Jan. 1988.

[17] C. Huang and E. H. W. Chan, "Photonics-based serrodyne microwave frequency translator with large spurious suppression and phase shifting capability," *J. Lightw. Technol.*, vol. 39, no. 7, pp. 2052–2058, Apr. 2021.

[18] M. I. Skolnik, *Radar Handbook*. New York, NY, USA: McGraw-Hill, 2008.